



Original Research

Effect of Heat Processing on the Quality of Ready-to-Eat Stinky Mandarin Fish and Estimation of the Associated Real-Time Shelf-Life Under Different Storage Temperatures

Wenjing Chu¹, Can Zhang¹, Xiaopu Ren¹, Yan Cheng¹, Fei Chen¹, Xiong Xiong², Yongxiang Wu^{1,*}

¹College of Life and Environment Sciences, Huangshan University, 245041 Huangshan, Anhui, China

²College of Food Science and Light Industry, Nanjing Tech University, 211816 Nanjing, Jiangsu, China

*Correspondence: wyx2009sun@aliyun.com (Yongxiang Wu)

Academic Editor: Corinna Kehrenberg

Submitted: 13 January 2026 Revised: 19 March 2026 Accepted: 24 March 2026 Published: 30 April 2026

Abstract

Background: Stinky mandarin fish (SMF) is a quintessential representative of traditional Chinese fermented fish products. With the advancement and widespread promotion of ready-to-eat (RTE) products, SMF is gradually transitioning from a regional catering product to a daily mass consumption food. However, the current literature is limited by a lack of systematic studies on the patterns of quality changes in RTE SMF during heat processing and storage at different temperatures. **Methods:** This study systematically analyzed quality changes in RTE SMF subjected to heat processing, specifically frying and sterilization, as well as storage at 20, 30, and 40 °C. **Results:** The optimal deep-frying conditions for RTE SMF were determined to be 200 °C for 3.5 min. Under these conditions, the product exhibited a moderate moisture content, a relatively low oil content, an appealing color. Moreover, the most favorable texture properties of RTE SMF were achieved through thermal sterilization at 115 °C for 14 min. TVB-N (total volatile basic nitrogen) was identified as the key indicator for predicting the shelf life of RTE SMF. Thus, a predictive model based on this indicator was successfully established and showed good agreement with the measured values, with the absolute relative error ranging from 3.19% to 6.74%. **Conclusions:** In summary, this study provides valuable data and a theoretical foundation for the further development of RTE SMF.

Keywords: RTE (ready-to-eat); SMF (stinky mandarin fish); heating processing; quality changes; total volatile basic nitrogen (TVB-N); shelf life

1. Introduction

Stinky mandarin fish (SMF) is a quintessential representative of traditional Chinese fermented fish products. It is crafted from fresh mandarin fish through a meticulous process of salt curing and fermentation, typically requiring subsequent culinary preparation before consumption [1]. Among the diverse regional variants of this product, Huizhou SMF is distinguished by its unique flavor profile, tender texture, and abundant nutritional benefits, making it a prominent symbol of Huizhou cuisine [2]. In recent years, Huizhou SMF has been officially recognized and included in the list of intangible cultural heritage.

With the advancement and promotion of ready-to-eat (RTE) products, SMF is progressively shifting from being a regional culinary specialty to a daily mass-consumed item, in line with the contemporary trend towards convenient food development [3]. However, despite the increasing market demand, systematic research on RTE-SMF remains relatively limited. In particular, existing studies predominantly focus on aspects such as optimization of the fermentation process [4], analysis of the microbial community [5,6], and the mechanisms of characteristic flavor compounds [7]. In contrast, there have been few investigations

into the quality change patterns of RTE-SMF undergoing heating processes, particularly frying and sterilization, as well as storage at various temperatures.

Deep-frying is a pivotal step in the preparation of RTE-SMF, endowing the fish chunks with a golden appearance. It also imparts a distinctive fried aroma and a desirable texture characterized by a crispy exterior and tender interior. Song *et al.* [8] found that the moisture content of pre-conditioned and clear-fried chum salmon gradually declined as the frying temperature increased and the frying time was prolonged. Ding *et al.* [9] compared the effects of two frying methods on the quality and flavor of hairtail. They observed that prolongation of the frying time intensified the surface color of fried hairtail so that it exhibited a tendency towards redness. Bhuiyan and Ngadi [10] investigated the influence of frying temperature and time on the quality of fried fish pieces coated with batter. Their experiments revealed that frying temperature had a significant impact on the a^* and b^* values, but no significant effect on the L^* value. Conversely, frying time had a significant impact on the L^* and b^* values, while having no significant effect on the a^* value. Furthermore, during the deep-frying process, the high temperature effectively inactivates any residual microbial flora that persists following fermentation of



the SMF, thereby exerting a bactericidal effect [11]. However, to our knowledge, there have been no in-depth studies on the impact of frying on the quality of RTE-SMF.

Another pivotal thermal processing technique that plays an indispensable role in guaranteeing the safety of RTE-SMF is thermal sterilization. This process can also have significant effects on the textural attributes of RTE-SMF, including elasticity, adhesiveness, hardness, and chewiness [12]. For instance, Zhu *et al.* [13] reported that the hardness of meat from *Takifugu rubripes* (pufferfish) tended to increase with rising temperature during heat treatment, ultimately leading to a tougher meat texture. Similarly, Chen *et al.* [14] found that at a constant roasting temperature of 120 °C, the hardness and chewability of roasted fillets from *Oreochromis niloticus* (tilapia) gradually increased with prolonged roasting time, while the elasticity decreased. Despite these findings, there remains a paucity of research on the thermal sterilization of RTE-SMF. Further in-depth investigation is needed to fully understand the alterations in textural characteristics of RTE-SMF induced by thermal sterilization.

Moreover, it is worth noting that during the storage of RTE-SMF, lipid oxidation and rancidity are prone to occur and can significantly compromise product quality and reduce the shelf life [15]. Storage temperature is a pivotal determinant in the deterioration of food quality. It holds significant practical relevance for the scientific prediction of shelf life, the formulation of rational storage strategies, and the assurance of product quality through systematic investigation of its impact on the storage quality of RTE-SMF. Previous studies have successfully established shelf-life prediction models for various aquatic products, including salmon [16] and bivalves [17], utilizing first-order kinetic models and Arrhenius equations. For instance, Li *et al.* [18] constructed a shelf life prediction model for crayfish products based on the core indicators of thiobarbituric acid and volatile basic nitrogen (TVB-N) level, predicting a shelf life of up to 10 days under ambient temperature conditions. Although the aforementioned research provides important background for predicting the shelf life of aquatic products, further investigation is needed to determine whether these experimental models and conclusions can be directly applied to RTE-SMF.

Based on these premises, the present study focused specifically on RTE-SMF. We systematically analyzed alterations in the quality of RTE-SMF following exposure to heating processes, specifically frying and sterilization, as well as storage at temperatures of 20 °C, 30 °C, and 40 °C. The moisture content, oil content, and color of RTE-SMF were quantified to investigate the effects of frying temperature and time. Moreover, we investigated the effects of temperature and time of thermal sterilization on the elasticity, adhesiveness, hardness, and chewiness of RTE-SMF. We also monitored changes in TVB-N, TPC (total plate count), AV (acid value), PoV (peroxide value), and SI (sensory in-

dex) under storage conditions of 20 °C, 30 °C, and 40 °C. Finally, we constructed a shelf-life prediction model by integrating a first-order reaction kinetics model with the Arrhenius equation. The results of this study provide valuable data and a theoretical foundation for the further advancement of RTE-SMF.

2. Materials and Methods

2.1 RTE-SMF Preparation

Frozen mandarin fish (about 500 g/piece) was purchased from Mount Huangshan Huimu Industrial Co., Ltd. To minimize individual variation, three mandarin fish were utilized to prepare the RTE-SMF samples as described by Chen *et al.* [7], with several modifications. Specifically, the frozen mandarin fish were thawed in tap water until they reached room temperature. The internal organs were then meticulously removed, and the fish were thoroughly rinsed with clean water to ensure the removal of any foreign matter. Subsequently, each fish was segmented into three parts, each measuring approximately 5 cm in length. These segments were then placed on a stainless-steel baking tray lined with silicone-coated paper. The baking tray was subsequently placed into an electric thermostatic drying oven set at 70 °C and dried for 90 min, with flipping at the 45 min mark to ensure uniform drying.

Based on the previous investigation, we have identified several key steps affecting the quality of RTE-SMF, including frying, sterilization and storage. Therefore, following the drying process, the fish segments were transferred to an electric deep-fryer set at a temperature range of 170–200 °C and fried for a duration of 3.5–5.5 min. Upon completion of the frying step, the fish segments were cooled to room temperature, vacuum-packed, and then heat sterilized. The sterilization temperatures employed were 100, 105, 110, 115, and 120 °C, with corresponding sterilization times of 5, 10, 15, 20, and 25 min, respectively. After sterilization, the samples were cooled to room temperature and stored in constant temperature incubators set at 20, 30, and 40 °C.

2.2 Determination of Water and Oil Content

The water content was determined using the direct drying method based on China's National Food Safety Standard (code GB 5009.3-2016) [19]. The fat content was determined according to the Soxhlet extraction method, as specified in China's National Food Safety Standard (code GB 5009.6-2025) [20], with the results expressed on a dry basis.

2.3 Color Analysis

The color properties were quantified utilizing a Minolta Chroma Meter CR-400 colorimeter (Konica Minolta Camera Co. Ltd., Tokyo, Japan). Chromaticity values (L^* , a^* , and b^*) for RTE-SMF that had been fried and cooled to room temperature were measured using a color difference

meter. Here, L^* represents the brightness value, a^* denotes the red-green value, and b^* indicates the yellow-blue value. Prior to measurement, calibration was performed using a white color plate. To ensure the rigor of the experiment, chromaticity was measured separately at five different parts of the fish block, and the average value of these five measurements was taken.

2.4 Texture Analysis

A modification of the method described by Fan *et al.* [21] was employed in the present study for texture analysis. Elasticity, adhesiveness, hardness, and chewiness were measured using a texture analyzer (Model TA-XT2, Texture Analyzer, Texture Technologies Corp., Scarsdale, NY, USA) equipped with a 36 mm flat-bottomed cylindrical probe. The measurement conditions were as follows: a pre-test speed of 60 mm/min, a test speed of 60 mm/min, a post-test speed of 60 mm/min, a compression degree of 30%, a distance of 1.00 mm, a trigger force of 0.03 N, and an automatic trigger type. After heat sterilization, RTE-SMF was removed and cooled to room temperature. The middle section of the fish was then selected for measurement. Each measurement involved two pieces of fish meat, with each piece being measured three times, resulting in a total of six measurements. The average of these measurements was subsequently calculated.

2.5 TVB-N Determination

The TVB-N content was extracted and measured as described by the Volatile Salt-Based Nitrogen in Foods specified in China's National Food Safety Standard (code GB 5009.228-2016) [22].

2.6 Microbiological Analysis

Gradient dilution of the sample was carried out in strict compliance with the sample dilution protocol specified in GB 4789.2-2022 [23]. Specifically, 1 mL of suitably diluted sample homogenate was aspirated using a pipette and evenly spread onto a total viable count test plate. For each dilution level, three parallel samples were prepared to ensure experimental reproducibility. Concurrently, a blank control was established by transferring 1 mL of sterile diluent onto a separate test plate to validate the experimental conditions. Subsequently, all plates were incubated in a constant temperature incubator set at 30 °C for a duration of 48 h, after which the colonies were counted and recorded.

2.7 Determination of AV and PoV

Oil samples were obtained according to the extraction method for solid oil described in China's National Food Safety Standard (code GB 5009.229-2025) [24]. The acid value (AV) was subsequently determined by hot ethanol titration. The peroxide value (PoV) was determined according to the titration method described in China's National Food Safety Standard (code GB 5009.227-2023) [25].

2.8 Sensory Analysis

The sensory index (SI) for RTE-SMF, including color, taste, aroma, texture, and overall acceptance, was evaluated using the hedonic method according to Wu *et al.* [26] by a panel of 10 trained evaluators following ethical guidelines. The panelists were asked to assign a score between 1 (Exu, extremely unacceptable) and 20 (Exa, extremely acceptable) for overall acceptance, between 1 (Exu) and 20 (Exa) for aroma, between 1 (Exu) and 20 (Exa) for texture, between 1 (Exu) and 20 (Exa) for color, and between 1 (Exu) and 20 (Exa) for taste. When the comprehensive score was <60 points, the sample was judged to reach the sensory rejection point.

2.9 Establishment of the Shelf-Life Prediction Model for RTE-SMF

The first-order dynamics model has been widely used in prediction models for the shelf-life of aquatic products, with the relevant kinetic equation shown in Eqn. 1.

$$B = B_0 e^{kt} \quad (1)$$

In this equation, B is the index value of the product on day t of storage; B_0 is the initial index value of the product; t is the storage time (days); and k is the reaction rate constant.

The Arrhenius equation is shown in Eqn. 2, with the logarithm of both sides taken to obtain Eqn. 3.

$$k = k_0 \exp\left(-\frac{E_a}{RT}\right) \quad (2)$$

$$\ln k = \ln k_0 - \frac{E_a}{RT} \quad (3)$$

In these equations, k is the reaction rate constant; k_0 is the pre-exponential factor; E_a is the activation energy (J/mol); R is the gas constant (8.314 J/(mol·K)); and T is the thermodynamic temperature (K).

According to Eqn. 3, $\ln k$ is linear with $1/T$, a slope of $-E_a/R$, and an intercept of $\ln k_0$. E_a and k_0 can be calculated through linear fitting with Origin 2022 software, (version 8.6, OriginLab Corporation, Northampton, MA, USA); The shelf-life prediction model for the product (4) is obtained by combining Eqn. 1 and Eqn. 2.

$$SL = \frac{\ln(B/B_0)}{k_0 \exp(-E_a/RT)} \quad (4)$$

In this equation, SL is the predicted shelf life.

2.10 Statistical Analysis

All statistical analyses in this study were conducted utilizing SPSS version 27 (SPSS Inc., Chicago, IL, USA). Duncan's multiple range test was used to compare differences among the means. Differences were considered statistically significant at the level of 5% ($p < 0.05$) and 1% ($p < 0.01$). Origin 2022 software was used for mapping, and Design Expert 13 software (Stat-Ease, Minneapolis, MN, USA); was used for the response surface test.

3. Results and Discussion

3.1 Effect of the Frying Process on the Water and Fat Content of RTE-SMF

As a traditional Chinese fermented fish products, SMF is distinguished by the unique flavor and aroma, the favorable texture and nutritional composition. During the preparation in the present study, the three fish used were selected to be highly homogeneous in terms of weight, length, and physiological status to minimize biological variability. This sample size is consistent with similar studies in this specific field [2,8], where the focus is on the processing technology rather than population-level biological variation.

Specifically, the water content of RTE-SMF is a pivotal factor influencing its texture and overall mouthfeel. Generally, an elevated moisture content correlates with enhanced tenderness, whereas a diminished content results in compromised palatability [27]. For a consistent frying duration, the moisture content decreased with rising temperature, albeit with notable variations across different time intervals (Fig. 1E–H). Specifically, at the 3.5 min mark, the moisture content decreased from 71.28% (170 °C) to 67.76% (200 °C), representing a 3.51% reduction. However, at 5.5 min, the decline was marginal (63.8% to 63.39%), equating to a decrease of just 0.41%. This difference may be due to the fact that prolonged frying facilitates greater oil adsorption into the pores left by evaporated water, thereby impeding further water seepage [28]. Notably, at 190 °C for 5.5 min, the moisture content reached a minimum of 62.16%, rendering the RTE-SMF significantly tougher. In contrast, at 200 °C, the moisture content showed minimal variation compared to other temperatures. Frying for 3.5 min at 200 °C yielded the highest moisture content and a tender texture, rendering it optimal for consumption.

The oil content of RTE-SMF plays a pivotal role in determining both the quality and shelf life. High-oil foods are inherently susceptible to oxidation processes, which may in turn increase the risks associated with cardiovascular diseases [29]. A notable increase in oil content was observed with prolonged frying duration across all tested temperatures (Fig. 1E–H). Specifically, at a temperature of 170 °C, the oil content increased significantly from 10.2% after 3.5 min of frying to 18.35% after 5.5 min ($p < 0.05$). This phenomenon could be attributed to the conversion of surface water into vapor at elevated temperatures, leading to the formation of pores that facilitate oil penetration, a finding

consistent with observations reported by He *et al.* (2026) [30]. Interestingly, at a higher temperature of 200 °C, the oil content exhibited minimal variation over time. At frying durations of 3.5 min and 4 min, the oil content was significantly lower, measuring 10.25% and 11.25%, respectively ($p < 0.05$). These results suggest that frying RTE-SMF at 200 °C for either 3.5 or 4.0 min is preferable for achieving a lower oil content, thereby potentially enhancing the overall quality and extending the shelf life.

3.2 Effect of the Frying Process on the Color of RTE-SMF

Alterations in food color stem predominantly from the Maillard reaction, caramelization, and other associated chemical reactions [31]. Diverse frying conditions elicit distinct color modifications in RTE-SMF. As the frying temperature and time increases, the brightness of RTE-SMF gradually diminishes, displaying varying patterns at different temperatures (Fig. 1). As shown in Fig. 1A–D, the L^* values of RTE-SMF fell significantly ($p < 0.05$) over time at 170 °C, 180 °C, and 190 °C. This phenomenon can be attributed to the acceleration of pigment-forming Maillard and caramelization reactions under high-temperature frying conditions [32]. Additionally, the evaporation of water during frying reduces light reflection, thereby contributing to the decreased L^* value. Conversely, at 200 °C, the L^* value initially declined from 37.42 (3.5 min) to 35.38 (4 min) and then remained stable ($p > 0.05$), indicating less impact of frying time on the L^* value at high temperature. The highest L^* value of 43.10 was observed at 170 °C for a frying duration of 3.5 min.

Moreover, RTE-SMF exhibited a yellowing phenomenon with rising temperature (Fig. 1). Under the same temperature conditions, the a^* value showed an upward trend with the prolongation of frying duration. Specifically, at 170 °C, the a^* value increased from 1.14 (at 3.5 min) to 2.68 (at 5.5 min), whereas at 200 °C it only increased from 1.64 (at 3.5 min) to 2.46 (at 5.5 min). Consequently, it can be inferred that the a^* value is more significantly influenced by the frying time at lower temperatures (Fig. 1A–D). The b^* value showed a time-dependent increase at 170 °C. In contrast, at 180 °C, 190 °C, and 200 °C, it showed an initial rise and then a subsequent decline. At 200 °C, the b^* values peaked at 15.82 (at 3.5 min) and 16.08 (at 4 min). These values were significantly higher compared to the other time points ($p < 0.05$), but then decreased to 11.28 as time progressed.

The observed color changes may be attributed to water evaporation, which creates pores that facilitate oil penetration and contribute to the formation of a golden hue [33]. Additionally, complex chemical reactions generate pigments that are responsible for the yellowing of RTE-SMF [34]. As both the temperature and time increase, the yellow coloration transitions to a reddish-brown shade, leading to an increase in the a^* value and a decrease in the b^* value. Therefore, when fried at 200 °C for either 3.5 min

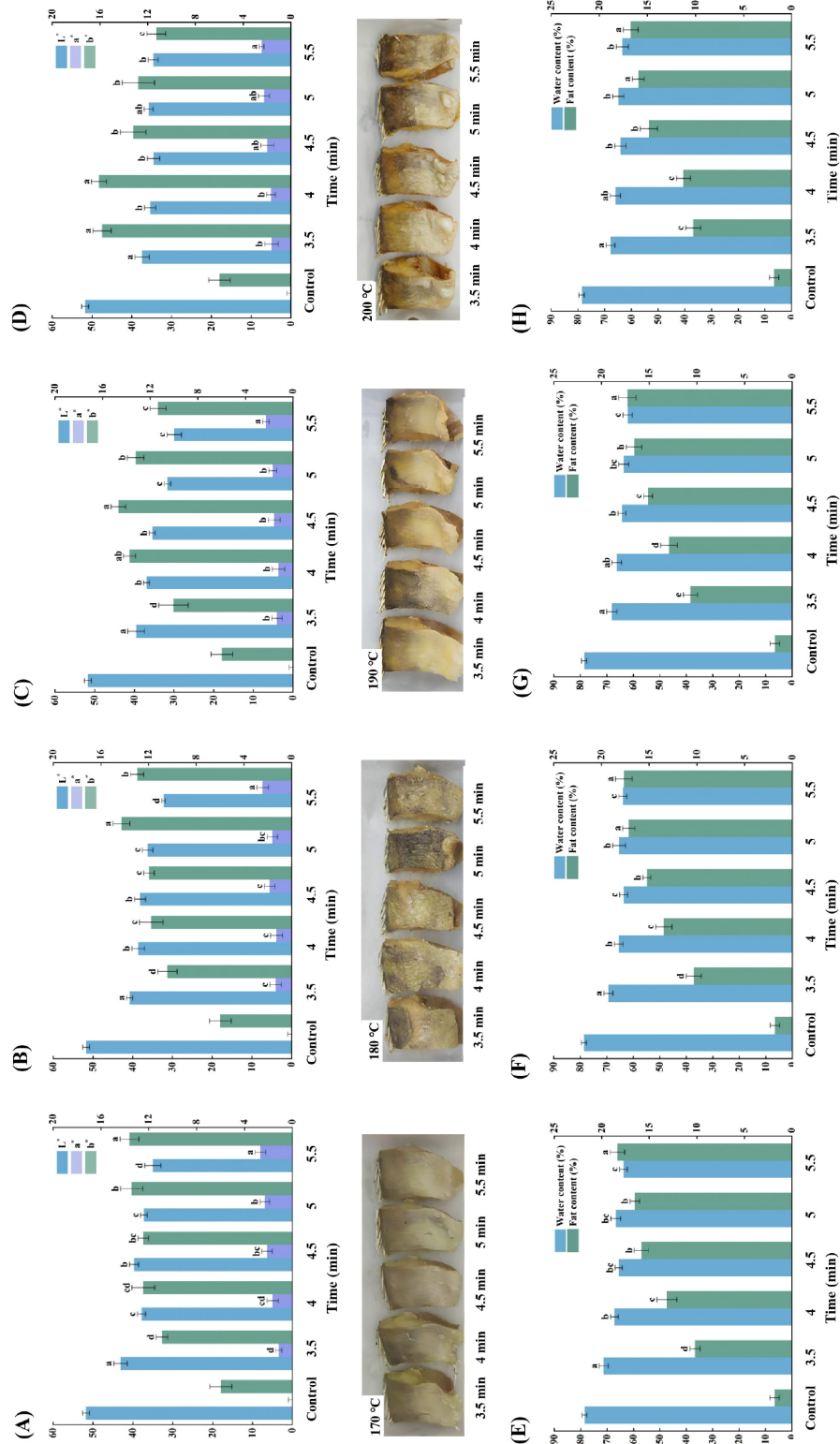


Fig. 1. Effect of frying temperature (170 °C, 180 °C, 190 °C, 200 °C) and frying time (3.5 min, 4 min, 4.5 min, 5 min, 5.5 min) on the quality of SMF (stinky mandarin fish). (A–D) described the color analysis, and (E–H) described the water content and fat content. For (A–D), the y-axis on the right represents the a* and b* values, and the y-axis on the left represents the L* value. For (E–H), the y-axis on the right represents the fat content, and the y-axis on the left represents the water content. (A) and (E) belong to the treatment of 170 °C. (B) and (F) belong to the treatment of 180 °C. (C) and (G) belong to the treatment of 190 °C. (D) and (H) belong to the treatment of 200 °C. Different letters (a, b, c, d) indicate significant difference at $p < 0.05$ (mean \pm standard deviation, $n = 3$).

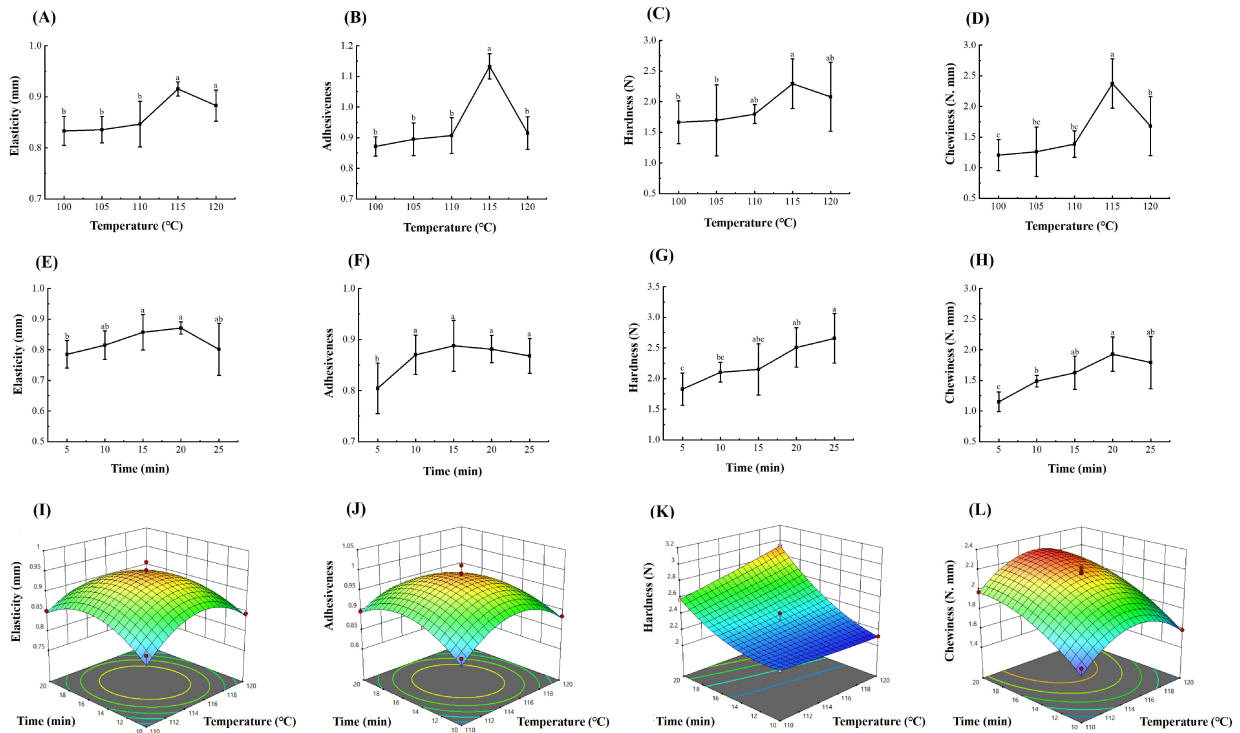


Fig. 2. Effect of thermal sterilization on the quality of SMF (stinky mandarin fish). (A–D) described the texture properties under different temperatures (100 °C, 105 °C, 110 °C, 115 °C, 120 °C) for 15 min. (E–H) described the texture properties under different heating periods (5 min, 10 min, 15 min, 20 min, 25 min) for 115 °C. (I–L) described the interactive effect of thermal sterilization temperature and time on texture characteristics using response surface analysis. Different letters (a, b, c) indicate significant difference at $p < 0.05$ (mean \pm standard deviation, $n = 3$).

or 4 min, RTE-SMF exhibits favorable brightness, a golden and uniform appearance, moderate L^* and a^* values, and a relatively high b^* value.

3.3 Effect of Thermal Sterilization on the Texture Characteristics of RTE-SMF

Texture properties are key indicators for assessing RTE-SMF quality, including elasticity, adhesiveness, hardness, and chewiness [35]. In particular, elasticity generally refers to tissue deformation and recovery under external force, while adhesiveness is the ability of RTE-SMF to resist damage during chewing and maintain integrity due to tight muscle fiber connections. Recent studies have demonstrated that higher elasticity and adhesiveness in fish meat can lead to a better mouthfeel [36]. Furthermore, hardness is the force needed for a certain deformation during the first sample compression, reflecting product firmness. Chewiness is the energy required to chew a solid sample into a stable state before swallowing. It is numerically equal to the product of elasticity, adhesiveness, and hardness, with complex change reasons.

After 15-min sterilization, the elasticity, adhesiveness, hardness, and chewiness of RTE-SMF at 115 °C were all significantly higher ($p < 0.05$) than at 100 °C, 105 °C, or 110 °C (Fig. 2A–D). For elasticity, this may be because high temperatures promote protein denaturation, forming a 3D

gel network that enhances elasticity. Alternatively, at 120 °C, the elasticity of RTE-SMF may decrease slightly due to water loss. Instead, high temperatures may induce collagen cross-linking or reorganize partially hydrolyzed products, thereby improving adhesiveness. At 120 °C, adhesiveness drops significantly ($p < 0.05$), possibly because higher temperatures loosen RTE-SMF. High temperatures may also reduce internal water, leading to muscle fiber contraction and higher protein density, thus raising hardness. Sakuyama *et al.* (2025) [37] suggested that thermal denaturation and cross-linking of fish protein strengthen intermolecular forces and increase product hardness. At 120 °C, hardness decreases slightly, perhaps because high temperature breaks the chemical bonds that maintain protein structures, leading to denaturation and tissue brittleness.

At a heat sterilization temperature of 115 °C, the elasticity of RTE-SMF increased significantly ($p < 0.05$) as the time extended from 5 and 10 min to 20 min, likely due to myofibrillar denaturation (Fig. 2E). The decreased elasticity observed at 25 min is probably because the excessive heating causes protein denaturation and contraction. The adhesiveness of RTE-SMF also increased significantly ($p < 0.05$) from 5 min to 10 min, peaking at 15 min (Fig. 2F). A possible reason could be that myofibrillar protein aggregation leads to gel formation. After 15 min, adhesiveness starts to decline due to water loss from the protein molecule

Table 1.1. Experimental design and response to texture characteristics (elasticity, adhesiveness, hardness, and chewiness) of stinky mandarin fish (SMF) with different thermal sterilization temperature and time.

Run	A: Temperature (°C)	B: Time (min)	Elasticity (mm)	Adhesiveness	Hardness (N)	Chewiness (N·mm)
1	110	10	0.835	0.875	2.186	1.592
2	120	10	0.845	0.885	2.116	1.584
3	110	20	0.852	0.897	2.576	1.975
4	120	20	0.798	0.845	2.927	1.970
5	108	15	0.800	0.851	2.246	1.533
6	122	15	0.815	0.854	2.429	1.681
7	115	8.0	0.820	0.868	2.143	1.545
8	115	22	0.846	0.896	3.008	2.278
9	115	15	0.953	0.992	2.284	2.164
10	115	15	0.930	0.974	2.408	2.180
11	115	15	0.973	1.012	2.254	2.220
12	115	15	0.934	0.969	2.312	2.107
13	115	15	0.940	0.985	2.308	2.144

Table 1.2. Regression equation of significant responses of SMF.

Response	Regression equation	R ²	F value	Adjusted R ²	p value
Y1: Elasticity	$Y1 = 0.9460 - 0.0028A + 0.0008B - 0.0160AB - 0.0662A^2 - 0.0534B^2$	0.9462	24.62	0.9078	0.0003
Y2: Adhesiveness	$Y2 = 0.9864 - 0.0047A + 0.0027B - 0.0155AB - 0.0649A^2 - 0.0501B^2$	0.9561	30.50	0.9248	0.0001
Y3: Hardness	$Y3 = 2.31 + 0.0675A + 0.3030B + 0.1053AB + 0.0108A^2 + 0.1298B^2$	0.9857	96.38	0.9755	<0.0001
Y4: Chewiness	$Y4 = 2.16 + 0.0245A + 0.2257B + 0.0008AB - 0.2728A^2 - 0.1205B^2$	0.9770	59.58	0.9606	<0.0001

network. At 115 °C, the hardness of RTE-SMF gradually increased with longer heat sterilization times (Fig. 2G). Prolonged sterilization likely causes more severe internal structural damage, causing loss of juice and increased hardness. Additionally, the chewiness of RTE-SMF gradually increased with longer sterilization times, but declined at 25 min (Fig. 2H).

Moreover, using elasticity, adhesiveness, hardness, and chewiness as evaluation indicators, the response surface test design was used to determine the optimal thermal sterilization parameters for RTE-SMF (results shown in Table 1.1). The regression equations derived for texture properties (elasticity, adhesiveness, hardness, and chewiness) as functions of the sterilization temperature and time were statistically significant, as indicated by the high R² values (from 0.9462 to 0.9857). Therefore, the models can explain a substantial portion of the variability in the response variables. In order to gain a more intuitive understanding of the interaction between sterilization temperature and time on each indicator, corresponding response surface plots were obtained based on the results of variance analysis in the regression model (Fig. 2I–L). As the sterilization temperature increased, the elasticity, adhesiveness, and chewiness of RTE-SMF showed a trend of initially increasing and then decreasing, while hardness showed no significant change ($p > 0.05$). Additionally, as the sterilization time increased, the elasticity and adhesiveness of RTE-SMF showed a trend of first increasing and then decreasing, while the hardness and chewiness continued to increase. Statistically significant interaction terms (e.g., temperature × time) in the re-

gression equations indicated that the effect of one factor (e.g., temperature) on the response variable (e.g., hardness) depended on the level of the other factor (e.g., time). This was crucial for identifying the optimal processing conditions, where small changes in both temperature and time could result in substantial improvements in texture. The 3D response surfaces for elasticity and adhesiveness were relatively flat, whereas the 3D response surfaces for hardness and chewiness were relatively steep. This indicates the temperature and time of thermal sterilization have no significant effect on elasticity and adhesiveness, but a significant effect on hardness and chewiness, consistent with the results of variance analysis (Table 1.2).

Accordingly, the optimal conditions for thermal sterilization were a temperature of 114.81 °C and a time of 13.99 min. Based on practical operations, the thermal sterilization parameters were therefore optimized to a temperature of 115 °C and a time of 14 min. Six validation tests were conducted under these conditions, with the average values for elasticity, adhesiveness, hardness, and chewiness found to be 0.929 mm, 0.965, 2.294 N, and 2.056 N·mm, respectively (Supplementary Table 1). The close proximity between the actual and predicted values indicates the reliability of the experimental model. Moreover, this sterilization intensity is compatible with standard retort systems commonly used in food processing, meeting well with the regulatory requirements for RTE foods in China, which could effectively ensure microbial safety while preserving the sensory and textural qualities of vacuum-packaged RTE-SMF.

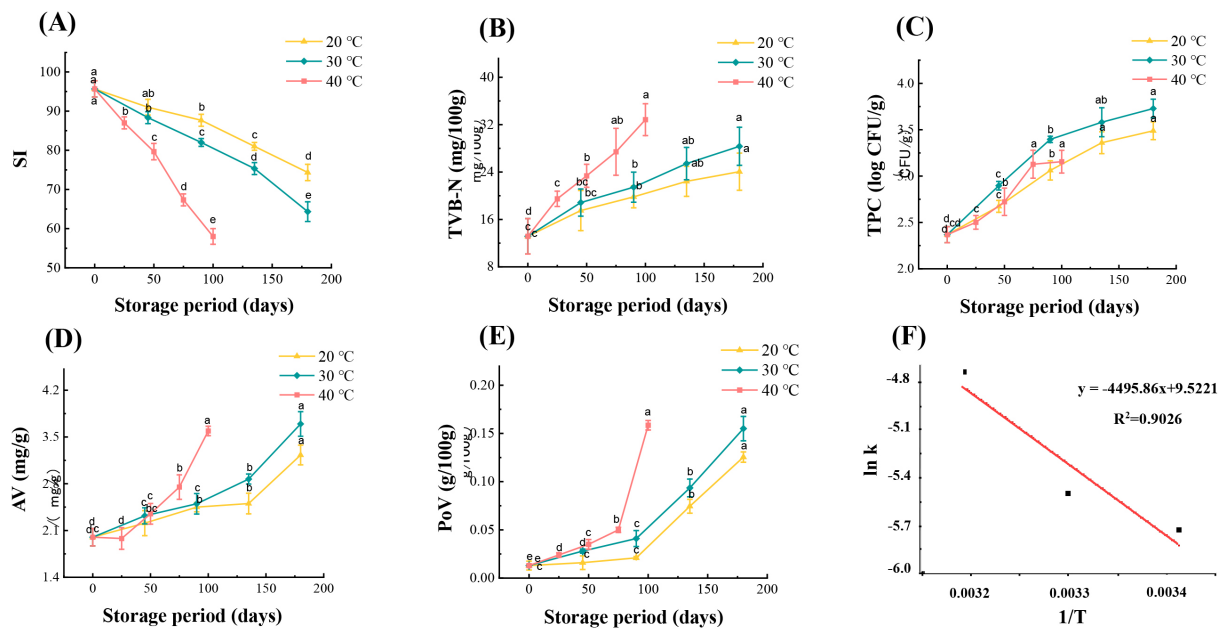


Fig. 3. Effect of different storage conditions on the quality of RTE (ready-to-eat) SMF (stinky mandarin fish). (A) Change with sensory index (SI). (B) Total volatile basic nitrogen (TVB-N). (C) Total plate count (TPC). (D) Acid value (AV). (E) Peroxide value (PoV) of RTE-SMF over time under different constant temperature storage conditions were described. (F) described the Arrhenius curve of TVB-N in RTE-SMF at different storage temperatures. Different letters (a, b, c, d) indicate significant difference at $p < 0.05$ (mean \pm standard deviation, $n = 3$).

3.4 Quality Changes in RTE-SMF During Storage

With the development and promotion of RTE products, SMF is gradually shifting from regional catering to daily consumption by the general public, in line with the trend of modern food convenience [38]. Therefore, it is important to comprehensively analyze the quality changes in RTE-SMF during storage and to predict its shelf life.

Sensory evaluation is an indispensable tool for quantifying food quality degradation, renowned for its directness and efficiency in capturing consumer-perceived attributes. As shown in Fig. 3A, the sensory acceptability of RTE-SMF exhibited a time-dependent decline under varying storage temperatures, with higher temperatures exacerbating the rate of deterioration. Specifically, at 40 °C, the SI had fallen to 58 points by day 100, breaching the consumer acceptability limit of 60 points. This decline manifested as pronounced darkening of the product's appearance, attenuation of its signature fresh and savory aroma, and the development of undesirable off-notes, collectively rendering the RTE-SMF unacceptable. Conversely, when stored for 175 days at 20 °C and 30 °C, the SI retained values of 74.3 and 64.3 points, respectively, thereby maintaining consumer acceptability.

TVB-N serves as a critical indicator for evaluating freshness and spoilage in aquatic products, originating from the enzymatic and microbial degradation of proteins into ammonia, amines, and other alkaline nitrogenous compounds [39]. As shown in Fig. 3B, the TVB-N content of RTE-SMF increased progressively with storage time across

all tested temperatures, with a more pronounced accumulation observed at elevated temperatures. Specifically, TVB-N reached 32.85 mg/100 g by day 100 at 40 °C, exceeding the regulatory threshold [40]. In contrast, after 180 days at 20 °C and 30 °C, TVB-N levels remained below the limit at 24.07 mg/100 g and 28.85 mg/100 g, respectively. These findings suggest that elevated storage temperatures expedite the accumulation of TVB-N, likely due to enhanced endogenous enzymatic activity and microbial proliferation accelerating protein degradation [39]. The temperature-sensitive nature of TVB-N production has also been reported with other aquatic products. For instance, in lightly salted salmon, TVB-N increased more rapidly at 25 °C than at lower temperatures (5 °C and 15 °C), reaching shelf-life endpoints as early as day 47 [41].

The TPC of RTE-SMF demonstrated a marked upward trajectory with prolonged storage duration (Fig. 3C). During the initial storage phase, TPC increased rapidly across all temperature groups, with the 40 °C group entering a stationary phase after 75 days. Throughout the entire storage period, the growth rate of TPC under 30 °C was notably higher than that under 20 °C. When the SI of samples declined to the rejection threshold, the corresponding TPC values were 3.49 log (CFU/g), 3.73 log (CFU/g), and 3.16 log (CFU/g) under storage conditions of 20 °C, 30 °C, and 40 °C, respectively. According to China's National Food Safety Standard (code GB 10136-2015) [40], the permissible limit for TPC in processed aquatic products is 5 log (CFU/g). The findings of this study indicate that even when

Table 2. Pearson correlation coefficients among various indicators of ready-to-eat (RTE) stinky mandarin fish (SMF) at different storage temperatures.

Storage temperature (°C)	Trait	SI	TVB-N	AV	PoV	TPC
20	SI	1	-0.962**	-0.953*	-0.956*	-0.962**
	TVB-N		1	0.884*	0.841	0.990**
	AV			1	0.928*	0.876
	PoV				1	0.851
	TPC					1
30	SI	1	-0.980**	-0.983**	-0.970**	-0.937*
	TVB-N		1	0.935*	0.919*	0.976**
	AV			1	0.989**	0.860
	PoV				1	0.833
	TPC					1
40	SI	1	-0.991**	-0.947*	-0.865	-0.978**
	TVB-N		1	0.921*	0.855	0.954*
	AV			1	0.963**	0.895*
	PoV				1	0.762
	TPC					1

Note: * $p < 0.05$, ** $p < 0.01$. SI, sensory index; TVB-N, total volatile basic nitrogen; AV, acid value; PoV, peroxide value; TPC, total plate count.

samples reached sensory unacceptability, their maximum TPC (3.73 log CFU/g) remained well below the regulatory threshold. The result supports the conclusion that from a microbiological perspective, RTE-SMF retains high food safety at the end of its shelf life.

AV has been widely acknowledged as an important indicator for assessing the degree of lipid hydrolysis, reflecting the free fatty acid (FFA) content of oils and fats. During storage, the lipids in RTE-SMF undergo progressive hydrolysis and oxidation, leading to the accumulation of FFAs and a consequent rise in AV. As shown in Fig. 3D, AV exhibited a significant upward trend with increasing storage time across all temperatures, aligning with a previous report on fried aquatic products [42]. During the initial storage phase (0–50 days), AV growth remained relatively slow across all temperature groups, with no significant differences observed among the groups by day 50. However, by the mid-to-late storage period, the temperature-dependent acceleration of AV elevation became pronounced, with higher temperatures being associated with more rapid increases. Notably, Effect of ultra high pressure on the bacterial community structure and quality of stinky mandarin fish after 100 days at 40 °C, whereas the corresponding values after 180 days at 20 °C and 30 °C were 3.23 mg/g and 3.70 mg/g, respectively. These results underscore the significant impact of storage temperature on AV accumulation. Lower temperatures could mitigate the rise in AV by suppressing microbial activity and the function of endogenous lipases, thereby attenuating the processes of lipid hydrolysis and FFA formation [42].

PoV serves as a critical marker for evaluating the initial oxidation stage of lipids, providing a clear indication of the accumulation of primary oxidation products. As shown

in Fig. 3E, the PoV of RTE-SMF increased significantly with prolonged storage time ($p < 0.05$). During the initial storage phase (0–50 days), the growth in PoV was relatively gradual across all temperature groups. However, a temperature-dependent acceleration of oxidation became apparent during the mid-to-late storage phase, with higher temperatures associated with a more rapid increase in PoV. In particular, at 40 °C, PoV increased from an initial 0.013 g/100 g to 0.156 g/100 g ($p < 0.05$) after 100 days, representing an approximately 11-fold increase. In contrast, after 180 days of storage at 20 °C and 30 °C, the PoV values reached 0.126 g/100 g and 0.155 g/100 g, respectively. These results demonstrate a substantial accumulation of primary oxidation products and accelerated lipid oxidation in the mid-to-late storage phase. This trend agrees with the AV results (Fig. 3D), collectively demonstrating the promoting effect of elevated temperature on lipid quality deterioration in RTE-SMF. Although samples stored at 40 °C for 100 days were deemed sensorially unacceptable, their PoV (0.156 g/100 g) remained far below the regulatory limit of 2.5 g/100 g specified in China’s National Food Safety Standard (code GB 10136-2015) [40].

3.5 Establishment and Validation of a Shelf-Life Model for RTE-SMF

Finally, we aimed to scientifically assess the key indicators for predicting the shelf life of RTE-SMF. We therefore performed Pearson correlation analysis between SI and TVB-N, AV, PoV, and TPC at different storage temperatures (Table 2). Across all temperatures, only TVB-N consistently showed a significant negative correlation with SI ($p < 0.01$), demonstrating optimal stability and reliability. Therefore, TVB-N was selected as a key indicator for eval-

Table 3. Kinetic parameters of TVB-N in ready-to-eat (RTE) stinky mandarin fish (SMF) at different storage temperatures.

Trait	Storage temperature (°C)	The first-order kinetic equation	The rate constant of reaction (k)	Coefficient of determination (R ²)
TVB-N	20	$y = 0.00324x + 2.65191$	0.00324	0.9335
	30	$y = 0.00408x + 2.66459$	0.00408	0.9438
	40	$y = 0.00869x + 2.66555$	0.00869	0.9595

Table 4. Comparison between predicted and actual shelf-life of RTE (ready-to-eat) SMF (stinky mandarin fish) at different storage temperatures.

Trait	Storage temperature (°C)	Predicted value (days)	Observed value (days)	Relative error (%)
TVB-N	20	278.56	270	3.19
	30	167.87	180	-6.74
	40	104.50	100	4.50

uating storage quality and predicting the shelf life of RTE-SMF. It was subsequently used for the construction of kinetic models. As shown in Table 3, the R² values of the TVB-N fitting equation under various temperatures all exceeded 0.93, indicating the first-order kinetic model faithfully describes the variation pattern of TVB-N during storage. Subsequently, the reaction rate constant (k) of TVB-N at different temperatures (shown in Table 3) was substituted into the Arrhenius equation, and a linear regression analysis was performed with 1/T as the x-axis and ln k as the y-axis. The R² value of the fitting equation was 0.9026, indicating a satisfactory fitting effect (Fig. 3F). The shelf-life prediction model based on TVB-N variation is shown in **Supplementary Fig. 1**. The predicted values from the model under various temperatures closely align with the measured values (Table 4). The relative error absolute value ranged between 3.19% and 6.74%. This is less than the acceptable error range of 10% commonly used for shelf-life prediction models, indicating our model has high prediction accuracy and reliability.

In real-world distribution chains, temperature fluctuations are common due to variations in ambient temperature, transportation conditions, and storage facilities. These fluctuations can significantly impact the rate of chemical reactions, including those responsible for TVB-N accumulation. Therefore, the model's predictions may need to be adjusted or validated under dynamic temperature conditions that more closely reflect real-world scenarios. Oxygen exposure is another critical factor affecting the shelf life of RTE-SMF. While the laboratory model may have controlled oxygen levels, in practice, variable oxygen exposure can be introduced by packaging materials, handling procedures, and storage conditions. To enhance the model's applicability, future studies should incorporate the oxygen permeability of packaging materials and simulate different oxygen exposure scenarios.

4. Conclusion

This study systematically analyzed the quality alterations in RTE-SMF subjected to frying and sterilization, as

well as storage at temperatures of 20, 30, and 40 °C. The optimal deep-frying conditions were found to be a temperature of 200 °C and a duration of 3.5 min. Moreover, the best texture properties of RTE-SMF were achieved under the thermal sterilization condition of 115 °C for 14 min. TVB-N exhibited the strongest correlation with SI and a significantly negative correlation at all temperatures. It was therefore selected as the key indicator for predicting the shelf life of RTE-SMF. A predictive model based on TVB-N was successfully constructed and showed good agreement with the measured values, with a relative error absolute value of 3.19%–6.74%. The results of this study provide valuable data and a theoretical foundation for the advancement of RTE-SMF.

Nevertheless, it should be noted that this model is based on constant laboratory conditions and may be affected by real-world fluctuations in environmental factors such as temperature, humidity, and light exposure. For instance, during transportation, the product may be exposed to extreme temperatures, either high due to direct sunlight or low in cold storage facilities with inconsistent temperature control. High humidity can promote microbial growth and accelerate chemical reactions that degrade the quality of the food product, while low humidity may cause the product to lose moisture and become dry and unpalatable. These real-world fluctuations can have a cumulative and interactive effect on the quality of RTE-SMF, potentially making the predictive model less accurate when applied outside the laboratory.

Moreover, future studies need to expand the number of experimental fish to at least six to better capture individual variations and enhance the external validity of the experiment. With a limited sample size, the study may not have accounted for the individual differences adequately, leading to results that may not be representative of the entire population of fish used for RTE-SMF production. Expanding the number of experimental fish to at least six, as suggested, would be a step in the right direction, but even larger sample sizes may be necessary to ensure that the findings are robust and can be generalized to a wider range of fish sources.

Availability of Data and Materials

Data sharing is not feasible in the present work due to participant confidentiality, and can only be available upon request.

Author Contributions

WJC, CZ and YXW designed the research study. WJC, CZ, XPR, YC, and FC performed the research. XX provided help and advice on the data analysis. XPR analyzed the predict model. WJC and YXW drafted the manuscript. All authors contributed to critical revision of the manuscript for important intellectual content. All authors read and approved the final manuscript. All authors have participated sufficiently in the work and agreed to be accountable for all aspects of the work.

Ethics Approval and Consent to Participate

Not applicable.

Acknowledgment

Not applicable.

Funding

This research was funded by Key projects of natural sciences in Colleges and universities of Anhui Province (2022AH051949), Huizhou stinky mandarin fish industry research institute project (HZCGY2025002), Anhui University Science and Technology Teachers Going to Enterprises to Practise Programme Project (2025jsqyg77, hxkt2025256), and Huangshan science and technology project (2023KN-03).

Conflicts of Interest

The authors declare no conflicts of interest.

Supplementary Material

Supplementary material associated with this article can be found, in the online version, at <https://doi.org/10.31083/JFSFQ49980>.

References

- [1] Guo KX, Hu B, Jiang Y, Li ZY, Qi J, Yu MM. Comprehensive insights into the mechanism of flavor formation in mandarin fish (*Siniperca chuatsi*) with inoculated fermentation. *Food Chemistry*. 2025; 479: 143717. <https://doi.org/10.1016/j.foodchem.2025.143717>.
- [2] Zhou BB, Wu ML, Jiang YY, Sun YX, Cui K, Lu JF. Flavoromics analysis of effects of fresh mandarin fish storage methods on Chouguiyu (Chinese fermented mandarin fish) flavor and microbial correlations. *Food Research International*. 2025; 221: 117226. <https://doi.org/10.1016/j.foodres.2025.117226>.
- [3] Xiao H, Feng TY, Yu J, Hu MY, Liu HY, Jiang XM, *et al*. Development of room-temperature fermented stinky sea bass and novel insights into its physicochemical and flavor formation and microbial diversity. *Food Bioscience*. 2023; 56: 103089. <https://doi.org/10.1016/j.fbio.2023.103089>.
- [4] Gao YX, Hou LZ, Gao J, Li DF, Tian ZL, Fan B, *et al*. Metabolomics approaches for the comprehensive evaluation of fermented foods: a review. *Foods*. 2021; 10: 2294. <https://doi.org/10.3390/foods10102294>.
- [5] Wang YQ, Chen Q, Li LH, Chen SJ, Zhao YQ, Li CS, *et al*. Transforming the fermented fish landscape: Microbiota enable novel, safe, flavorful, and healthy products for modern consumers. *Comprehensive Reviews in Food Science and Food Safety*. 2023; 22: 3560–3601. <https://doi.org/10.1111/1541-4337.13208>.
- [6] Belleggia L, Osimani A. Fermented fish and fermented fish-based products, an ever-growing source of microbial diversity: a literature review. *Food Research International*. 2023; 172: 113112. <https://doi.org/10.1016/j.foodres.2023.113112>.
- [7] Chen JN, Zhang YY, Huang XH, Dong M, Dong XP, Zhou DY, *et al*. Integrated volatolomics and metabolomics analysis reveals the characteristic flavor formation in Chouguiyu, a traditional fermented mandarin fish of China. *Food Chemistry*. 2023; 418: 135874. <https://doi.org/10.1016/j.foodchem.2023.135874>.
- [8] Song GS, Zeng MW, Chen SJ, Lyu ZF, Jiang NL, Wang DL, *et al*. Exploring molecular mechanisms underlying changes in lipid fingerprinting of salmon (*Salmo salar*) during air frying integrating machine learning-guided REIMS and lipidomics analysis. *Food Chemistry*. 2024; 460: 140770. <https://doi.org/10.1016/j.foodchem.2024.140770>.
- [9] Ding YX, Zhou T, Liao YQ, Lin HM, Zhang Bin, Deng SG, *et al*. Influence of two frying methods on the quality and flavor of hairtail. *Science and Technology of Food Industry*. 2022; 43: 244–253. <https://doi.org/10.13386/j.issn1002-0306.2022030023>. (In Chinese)
- [10] Bhuiyan MHR, Ngadi M. Application of batter coating for modulating oil, texture and structure of fried foods: a review. *Food Chemistry*. 2024; 453: 139655. <https://doi.org/10.1016/j.foodchem.2024.139655>.
- [11] Rim J, Kim DK. Bactericidal action of syringic acid and mild heat involving stress response in foodborne pathogens. *Food Bioscience*. 2025; 74: 107995. <https://doi.org/10.1016/j.fbio.2025.107995>.
- [12] Wang S, Lin SY, Li S, Qian XX, Li CQ, Sun N. Decoding the textural deterioration of ready-to-eat shrimp: Insights from dynamic myofibrillar protein changes during thermal sterilization. *Food Research International*. 2025; 202: 115745. <https://doi.org/10.1016/j.foodres.2025.115745>.
- [13] Zhu Y, Chen XT, Pan N, Liu SJ, Su YC, Xiao MT, *et al*. The effects of five different drying methods on the quality of semi-dried Takifugu obscurus filets. *LWT*. 2022; 161: 113340. <https://doi.org/10.1016/j.lwt.2022.113340>.
- [14] Chen JH, Shi CP, Xu JM, Wang XC, Zhong J. Correlation between physicochemical properties and volatile compound profiles in tilapia muscles subjected to four different thermal processing techniques. *Food Chemistry: X*. 2023; 18: 100748. <https://doi.org/10.1016/j.fochx.2023.100748>.
- [15] Wahab A, Suhag R, Ferrentino G, Morozova K, Scampicchio M. Oxidation kinetics of fats from meat and meat products by isothermal calorimetry. *Food Chemistry*. 2025; 478: 143653. <https://doi.org/10.1016/j.foodchem.2025.143653>.
- [16] Hua Q, Wang JW, Li D. Enhancement of microbial safety and shelf life of salmon filets by *Lactiplantibacillus plantarum* 299 V fermented in pomelo (*Citrus maxima*) peel extract. *Food Packaging and Shelf Life*. 2024; 46: 101359. <https://doi.org/10.1016/j.fpsl.2024.101359>.
- [17] Yuan Y, Lin SY, Dong XP, Liu B, Dong HY, Qiang JX, *et al*. Construction of a multilayer perceptron based intelligent platform for dynamic quality monitoring and shelf-life prediction of bivalves. *Food Chemistry*. 2026; 502: 147717. <https://doi.org/10.1016/j.foodchem.2025.147717>.

- [18] Li Q, Lei JY, Su KY, Chen XY, Cheng LH, Yang CM, *et al.* Processing and shelf-life prediction models for ready-to-eat crayfish. *Foods*. 2025; 14: 1296. <https://doi.org/10.3390/food14081296>.
- [19] National Health and Family Planning Commission of the People's Republic of China. GB 5009.3 - 2016. National food safety standard - Determination of moisture in foods. 2016. Available at: <https://sppt.cfsa.net.cn:8086/db> (Accessed: 20 December 2025).
- [20] National Health Commission of the People's Republic of China, State Administration for Market Regulation. GB 5009.6-2025 National food safety standard - Determination of fat in foods. 2025. Available at: <https://sppt.cfsa.net.cn:8086/db> (Accessed: 20 December 2025).
- [21] Fan HL, Fan DM, Huang JL, Zhao JX, Yan BW, Ma SY, *et al.* Cooking evaluation of crayfish (*Procambarus clarkia*) subjected to microwave and conduction heating: a visualized strategy to understand the heat-induced quality changes of food. *Innovative Food Science & Emerging Technologies*. 2020; 62: 102368. <https://doi.org/10.1016/j.ifset.2020.102368>.
- [22] National Health and Family Planning Commission of the People's Republic of China. GB 5009.228-2016 National food safety standard - Determination of volatile basic nitrogen in foods. 2016. Available at: <https://sppt.cfsa.net.cn:8086/db> (Accessed: 20 December 2025).
- [23] National Health Commission of the People's Republic of China, State Administration for Market Regulation. GB 4789.2-2022 National food safety standard - Food microbiological examination - Aerobic plate count. 2022. Available at: <https://sppt.cfsa.net.cn:8086/db> (Accessed: 20 December 2025).
- [24] National Health Commission of the People's Republic of China, State Administration for Market Regulation. GB 5009.229-2025 National food safety standard - Determination of acid value of foods. 2025. Available at: <https://sppt.cfsa.net.cn:8086/db> (Accessed: 20 December 2025).
- [25] National Health Commission of the People's Republic of China, State Administration for Market Regulation. GB 5009.227-2023 National food safety standard - Determination of peroxide value in foods. 2023. Available at: <https://sppt.cfsa.net.cn:8086/db> (Accessed: 20 December 2025).
- [26] Wu YX, Wang Y, Yuan DX, Zhang JX, Chu LM, Wang TT, *et al.* Effect of ultra high pressure on the bacterial community structure and quality of stinky mandarin fish. *Food Science*. 2022; 43: 81–87. <https://doi.org/10.7506/spkx1002-6630-20210208-144>. (In Chinese)
- [27] Zhang JW, Du DD, Xu YJ, Wang ZM, Cai KZ, Zeng QM, *et al.* Dynamic changes of tenderness, moisture and protein in marinated chicken: the effect of different steaming temperatures. *Journal of the science of food and agriculture*. 2024; 104 (12): 7668-7677. <https://doi.org/10.1002/jsfa.13603>.
- [28] Zhang SY, Gong ZG, Wang SM, Zhao SL, Mao W, Liu B, *et al.* Comprehensive insights into oil absorption in fried foods: The role of surface characteristics. *Food Chemistry*. 2025; 483: 144341. <https://doi.org/10.1016/j.foodchem.2025.144341>.
- [29] Costa-Beber LC, Goettens-Fiorin PB, dos Santos JB, Friske PT, Frizzo MN, Heck TG, *et al.* Air pollution combined with high-fat feeding aggravates metabolic and cardiovascular diseases: a dangerous, oxidative, and immune-inflammatory association. *Life Sciences*. 2023; 317: 121468. <https://doi.org/10.1016/j.lfs.2023.121468>.
- [30] He XY, Teng ZN, Chen JW, Feng JQ, Liao E, Wang Q. A new insight on oil penetration of breaded fish nuggets during deep-fat frying based on the surfactant effect. *Journal of Food Engineering*. 2026; 404: 112763. <https://doi.org/10.1016/j.jfoodeng.2025.112763>.
- [31] Wang SH, Bu QM, Feng Y. Non-targeted metabolomics reveals substrates and products of maillard reaction related to changes of color and aroma of dried sweet potato during storage. *Food Chemistry: X*. 2025; 31: 103031. <https://doi.org/10.1016/j.fochx.2025.103031>.
- [32] Liu YX, Liu C, Huang XS, Li MY, Zhao GM, Sun LX, *et al.* Exploring the role of Maillard reaction and lipid oxidation in the advanced glycation end products of batter-coated meat products during frying. *Food Research International*. 2024; 178: 113901. <https://doi.org/10.1016/j.foodres.2023.113901>.
- [33] Wang HS, Xu QL, Zhang TY, Liu JX, Zeng XQ, Li J, *et al.* Color dynamics and stabilization strategies in meat substitutes: Mechanistic insights and challenges in enhancing natural pigments. *Food Bioscience*. 2025; 73: 107609. <https://doi.org/10.1016/j.fbio.2025.107609>.
- [34] Pujol A, Ospina-E JC, Alvarez H, Muñoz DA. Myoglobin content and oxidative status to understand meat products' color: Phenomenological based model. *Journal of Food Engineering*. 2023; 348: 111439. <https://doi.org/10.1016/j.jfoodeng.2023.111439>.
- [35] Xiao H, Yu J, Hu MY, Liu HY, Yuan ZC, Xue Y, *et al.* Development of novel fermented stinky sea bass and analysis of its taste active compounds, flavor compounds, and quality. *Food Chemistry*. 2023; 401: 134186. <https://doi.org/10.1016/j.foodchem.2022.134186>.
- [36] Sharma S, Yadav KK, Ngasotter S, Gulati R, Bhalavey P, Yadav RP, *et al.* Emulsion-based strategies to enhance the physicochemical and structural properties of fish surimi: a comprehensive review. *Food Research International*. 2026; 226: 118242. <https://doi.org/10.1016/j.foodres.2025.118242>.
- [37] Sakuyama M, Kominami Y, Hayashi T, Ushio H. Protein structural and textural characteristics of sous-vide cooked rainbow trout (*Oncorhynchus mykiss*) meat. *International Journal of Gastronomy and Food Science*. 2025; 42: 101313. <https://doi.org/10.1016/j.ijgfs.2025.101313>.
- [38] Martins IBA, Alcantara M, Torrezan R, Tonon RV, da Matta VM, Deliza R. Investigating the eating patterns and expectations for the 60+: Insights for the development of new "ready-to-eat" products. *Food Quality and Preference*. 2025; 126: 105423. <https://doi.org/10.1016/j.foodqual.2024.105423>.
- [39] Lv YF, Yu ZQ, Li Y, Ye BB, Li JR, Li XP. Innovative application of a pH-sensitive indicator film: Monitoring the freshness of *Larimichthys crocea* based on the correlation model between hue value and TVB-N content. *Food Control*. 2026; 183: 111919. <https://doi.org/10.1016/j.foodcont.2025.111919>.
- [40] National Health and Family Planning Commission of the People's Republic of China (or relevant successor, e.g., National Health Commission), State Administration for Market Regulation. GB 10136-2015 National food safety standard - Aquatic products of animal origin. 2015. Available at: <https://sppt.cfsa.net.cn:8086/db> (Accessed: 20 December 2025).
- [41] Guo MQ, Lin H, Wang KQ, Cao LM, Sui JX. Data fusion of near-infrared and Raman spectroscopy: an innovative tool for non-destructive prediction of the TVB-N content of salmon samples. *Food Research International*. 2024; 189: 114564. <https://doi.org/10.1016/j.foodres.2024.114564>.
- [42] Li MY, Zhang MY, Chen HL, Du HY. Chemical quality indices, microbial community shifts, and biogenic amine exposure risk in boiled and fried ready-to-eat crayfish during refrigerated storage. *Journal of Food Composition and Analysis*. 2025; 143: 107585. <https://doi.org/10.1016/j.jfca.2025.107585>.